International Conference on Mathematics, Computational Methods & Reactor Physics (M&C 2009)
Saratoga Springs, New York, May 3-7, 2009, on CD-ROM, American Nuclear Society, LaGrange Park, IL (2009)

ANISOTROPIC DIFFUSION IN MODEL 2-D PEBBLE-BED REACTOR CORES

Richard Vasques
Department of Mathematics
University of Michigan
Ann Arbor, Michigan 48109 USA
rvasques@umich.edu

Edward W. Larsen
Department of Nuclear Engineering and Radiological Sciences
University of Michigan
Ann Arbor, Michigan 48109 USA
edlarsen@umich.edu

ABSTRACT

We describe an analysis of neutron transport in a modeled 2-D (transport in a plane) pebble-bed reactor (PBR) core consisting of fuel discs stochastically piled up in a square box. Specifically, we consider the question of whether the force of gravity, which plays a role in this piling, affects the neutron transport within the system. Monte Carlo codes were developed for (i) deriving realizations of the 2-D core, and (ii) performing 2-D neutron transport inside the heterogeneous core; results from these simulations are presented. In addition to numerical results, we present preliminary findings from a new theory that generalizes the atomic mix approximation for PBR problems. This theory utilizes a non-classical form of the Boltzmann equation in which the locations of the scattering centers in the system are correlated and the distance to collision is not exponentially distributed. We take the diffusion limit of this equation and derive an anisotropic diffusion equation. (The diffusion is anisotropic because the mean and mean-square distances between collisions in the horizontal and vertical directions are slightly different.) We show that the results predicted using the new theory more closely agree with experiment than the atomic mix results. We conclude by discussing plans to extend the present work to 3-D problems, in which we expect the anisotropic diffusion to be more pronounced.

Key Words: particle transport, random media, pebble-bed reactor, monte carlo

1. INTRODUCTION

The pebble bed reactor (PBR) is a graphite-moderated, gas-cooled, very high temperature reactor. It uses spherical, roughly tennis-ball-sized fuel elements called *pebbles*, which are made of pyrolytic graphite (the moderator), containing thousands of microscopic fuel Tristructural-isotropic (TRISO) particles, each of which consists of a fissile material surrounded by a coated ceramic layer of SiC for structural integrity. Thousands of pebbles are placed together in the PBR core, which is cooled by an inert or semi-inert gas such as helium.

Inside the PBR core, the fuel pebbles are piled on top of one another in a “random” manner. Typically, the neutronic modeling of the geometrically “random” core is done by: (i) developing self-shielded multigroup cross sections for the pebbles, (ii) volume-averaging these cross sections over the entire core, including the helium-filled region between the pebbles (the *atomic mix* approximation), and (iii) introducing the spatially-homogenized cross sections into a diffusion code.

This procedure suggests two questions that we have considered in our work. First, in the classic atomic mix approximation, the cross sections for a random heterogeneous medium are approximated by volume-averaging over the constituent materials, weighted by their respective volume fractions. This approximation is known to be accurate only when the *chunk sizes* of the constituent materials are small compared to a mean free path. However, PBR pebbles are not optically thin – they are O(1) mean free paths thick. This casts some doubt on the validity of the atomic mix approximation for PBRs: how accurate is it, really? The second question is related but subtly different: in a PBR core, does gravity affect the distance-to-collision, or chord length probability distribution function, in a direction-dependent (anisotropic) manner? In other words, the force of gravity (let us say it acts in the -z direction) causes the pebbles to become arranged in a certain manner. If one considers a typical arrangement of pebbles in a PBR core, is the chord length probability distribution function different in the z direction than in the (x, y)-plane? If it is different, neutron transport and diffusion can be affected in an anisotropic manner that is not modeled by the atomic mix approximation.

Currently, PBR cores are simulated using a diffusion approximation with an *isotropic* diffusion tensor, in which neutrons diffuse equally in all spatial directions. However, if the chord length probability distribution function is different in the z direction than in the x, y directions, then the diffusion length in the z direction could be different than in the x and y directions, and in this case one has an anisotropic diffusion tensor.

In this preliminary work, we consider a 2-D "flatland" (neutron transport occurs only in a plane) model of a PBR core, consisting of circular discs randomly piled up (by gravity) inside a box. (Hereafter, we use the term "2-D" to describe this model.) We have developed a Monte Carlo computer code to derive realizations of the 2-D core; and a second Monte Carlo code that performs 2-D neutron transport inside the heterogeneous core. By calculating neutron transport Monte Carlo simulations in the heterogeneous cores, we can determine (i) the accuracy of the atomic mix approximation, and (ii) whether anisotropic effects occur.

Our 2-D simulations show that the atomic mix model is reasonably accurate. However, there are small but discernible differences between the Monte Carlo results and the atomic mix model. In particular, we observe small anisotropic effects: neutron transport in the horizontal (x) direction slightly differs from that in the vertical (y) direction, in which the force of gravity acts. The classic atomic mix model does not account for this.

In addition to our numerical results, we present some preliminary results from a new and more accurate theory that generalizes the atomic mix approximation for PBR-type problems, with the inclusion of anisotropic behavior.

In Section 2 of this paper, we describe our numerical comparisons between the heterogeneous and atomic mix PBR cores. In Section 3, we present the new theory for a general, 3-D problem. In Section 4, we show that for the 2-D model presented here the new theory is more accurate than atomic mix. We conclude with a brief discussion in Section 5.

2 THE 2-D "FLATLAND" PROBLEM AND NUMERICAL RESULTS

We define material 1 as the background material (void) and material 2 as the material of the fuel discs (of radius r). In this case, for $i \in \{1, 2\}$ we have:

$$\Sigma_{ti} = \text{total cross section of material } i \ , \tag{1a}$$

$$c_i = \text{scattering ratio of material } i \ . \tag{1b}$$

In the following approach, we focus on the transport of the particles generated by a single fuel disc, since the particles generated by different discs will have (on average) the same behavior. To minimize the statistical error and obtain a general result we used the following procedure:

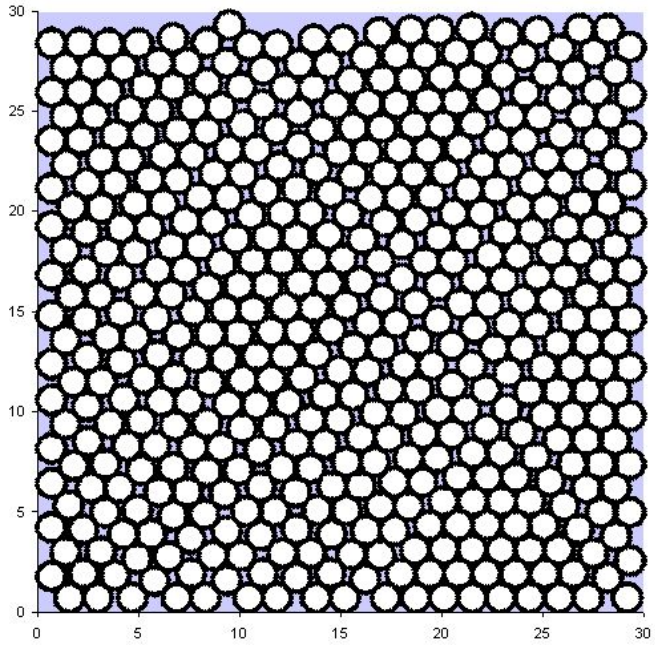

Figure 1. Packing of discs in a 30X30 box

$(\boldsymbol{a})$ A realization of the packed system is generated using the ballistic deposition model [1], adapted for the 2-D case (Fig. 1);

$(\boldsymbol{b})$ A disc D_0 close to the center of this system is chosen as the one in which particles will be generated;

$(\boldsymbol{c})$ A particle P is born randomly at a point inside D_0, with a random (2-D) direction of flight. Using Monte Carlo, we follow the history of the particle P and store all relevant information (such as distances travelled between collisions, distance from birth point to point of "death", etc.);

$(\boldsymbol{d})$ We repeat step $(\boldsymbol{c})$ for N_p particles;

$(\boldsymbol{e})$ We return to step $(\boldsymbol{a})$ and repeat the procedure for N_r different realizations of the system.

In the test problem presented here, we have a system of width $X = 200$ cm and height $Y = 200$ cm, with vacuum as the background material (material 1) and fuel discs of radius $r = 0.5$ cm (material 2), whose total cross section and scattering ratio are, respectively, $\Sigma_{t2} = 1.0$ cm^{-1} and $c_2 = 0.99$. The scattering in material 2 is assumed to be isotropic. The quantities we are interested in analyzing are:

$$\langle s \rangle = \text{mean distance to collision} , \tag{2a}$$
$$\langle s^2 \rangle = \text{mean-squared distance to collision} , \tag{2b}$$
$$\langle x^2 \rangle = \text{mean-squared horizontal distance to absorption (from point of birth)} , \tag{2c}$$
$$\langle y^2 \rangle = \text{mean-squared vertical distance to absorption (from point of birth)} , \tag{2d}$$
$$\langle \rho \rangle = \langle \sqrt{x^2 + y^2} \rangle = \text{mean distance to absorption (from point of birth)} , \tag{2e}$$
$$\langle \rho^2 \rangle = \langle x^2 + y^2 \rangle = \text{mean-squared distance to absorption (from point of birth)} . \tag{2f}$$

In our numerical simulations, we constructed $N_r = 600$ realizations of the system and generated $N_p = 2,000$ particles histories for each realization. This yields a total of $1,200,000$ simulated particles (of which only 57 ended up leaking out of the system). The average number of discs packed in each realization was found to be 41,541, which gives an average packing fraction $\langle \text{pack} \rangle \approx 0.81566$.

To obtain a theoretical prediction using the atomic mix model, we need the problem's parameters and the average packing fraction. With this information, we calculate

$$\langle \Sigma_t \rangle = \text{volume-averaged total cross section} = (1 - \langle \text{pack} \rangle)\Sigma_{t1} + \langle \text{pack} \rangle \Sigma_{t2} \tag{3a}$$

and

$$\langle c\Sigma_t \rangle = \text{volume-averaged scattering cross section} = (1 - \langle \text{pack} \rangle)c_1\Sigma_{t1} + \langle \text{pack} \rangle c_2\Sigma_{t2} \ . \tag{3b}$$

The atomic mix model assumes classical transport (in which the probability distribution function of the distance travelled between collisions is an exponential). In this case, $\langle s \rangle = 1/\langle \Sigma_t \rangle$ and $\langle s^2 \rangle^{1/2} = \sqrt{2}\langle s \rangle$.

The atomic mix equation [2] for this system with a point source at the origin is:

$$\boldsymbol{\Omega} \cdot \boldsymbol{\nabla} \langle \psi(\boldsymbol{x}, \boldsymbol{\Omega}) \rangle + \langle \Sigma_t \rangle \langle \psi(\boldsymbol{x}, \boldsymbol{\Omega}) \rangle = \frac{\langle c\Sigma_t \rangle}{2\pi} \langle \Phi(\boldsymbol{x}) \rangle + \frac{\langle Q(\boldsymbol{x}) \rangle}{2\pi} \delta(x)\delta(y) \ , \tag{4}$$

where $\boldsymbol{\Omega} = (\cos\varphi, \sin\varphi)$ and $\langle \Phi(\boldsymbol{x}) \rangle = \int_0^{2\pi} \langle \psi(\boldsymbol{x}, \boldsymbol{\Omega}) \rangle d\varphi$. Defining $\langle \Sigma_a \rangle = \langle \Sigma_t \rangle - \langle c\Sigma_t \rangle$, the classic diffusion equation for Eq. (4) is

$$-\frac{1}{2\langle \Sigma_t \rangle} \nabla^2 \langle \Phi(\boldsymbol{x}) \rangle + \langle \Sigma_a \rangle \langle \Phi(\boldsymbol{x}) \rangle = \langle Q(\boldsymbol{x}) \rangle \delta(x)\delta(y) \ . \tag{5}$$

(The factor 2 occurs in the diffusion coefficient because diffusion occurs only in a plane.)

To calculate the mean-squared distance of a particle from its birth point, we operate on Eq. (5) by $\int_{-\infty}^{\infty} \int_{-\infty}^{\infty} (x^2 + y^2)(\cdot) dx dy$ and get explicitly:

$$\frac{\int_{-\infty}^{\infty} \int_{-\infty}^{\infty} (x^2 + y^2) \langle \Phi(\boldsymbol{x}) \rangle dx dy}{\int_{-\infty}^{\infty} \int_{-\infty}^{\infty} \langle \Phi(\boldsymbol{x}) \rangle dx dy} = \langle \rho^2 \rangle = \frac{2}{\langle \Sigma_t \rangle \langle \Sigma_a \rangle} \ ; \tag{6}$$

similarly we can get $\langle x^2 \rangle = \langle y^2 \rangle = 1/(\langle \Sigma_t \rangle \langle \Sigma_a \rangle)$. The relative statistical errors for the numerical results (estimated using the Central Limit Theorem) and the relative errors of the atomic mix prediction compared to the numerical results are shown in Table I. The number of particles simulated guarantees that the statistical errors are smaller than the difference between the atomic mix prediction and the numerical results.

Table I. Numerical Results and Predictions of the Atomic Mix Model

	Numerical Results	Atomic Mix	Statistical Error (95% confidence)	Relative Error (Compared to Numerical Results)
$\langle s \rangle$	1.22127	1.22601	0.01859%	0.38748%
$\langle s^2 \rangle^{1/2}$	1.74365	1.73383	0.02068%	0.56318%
$\langle \rho^2 \rangle^{1/2}$	17.42908	17.33835	0.15929%	0.52056%
$\langle x^2 \rangle^{1/2}$	12.29878	12.26006	0.20612%	0.31479%
$\langle y^2 \rangle^{1/2}$	12.34961	12.26006	0.20503%	0.72507%

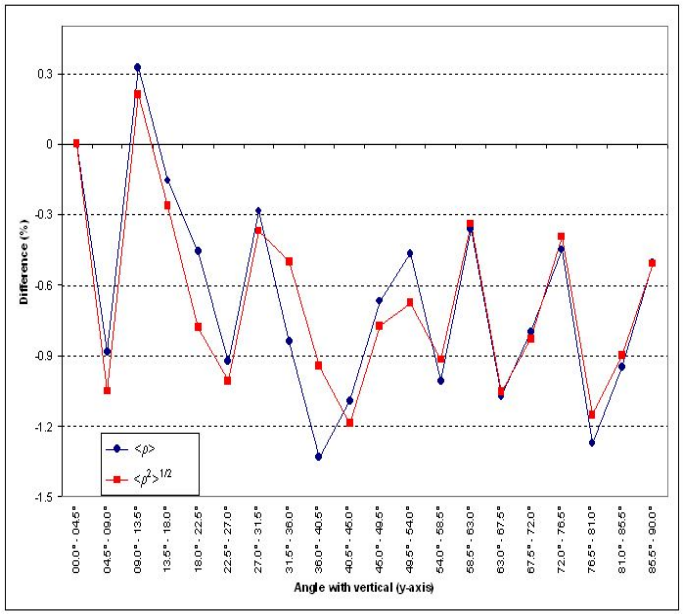

Figure 2. $\langle\rho\rangle$ and $\langle\rho^2\rangle^{1/2}$ at different angles

Another interesting trend is that $\langle x^2\rangle^{1/2}$ is about 0.42% smaller than $\langle y^2\rangle^{1/2}$. This indicates a small tendency of particles to travel further in the vertical direction than in the horizontal direction, which suggests that transport in this system has a small anisotropic behavior. To investigate this, we calculated the values of both $\langle\rho\rangle$ and $\langle\rho^2\rangle^{1/2}$ at different angular intervals formed with the vertical axis (each interval covering $4.5°$). In other words, we computed the mean and mean-squared distances to absorption (from point of birth) in different directions. The differences between these results and those obtained for the near-vertical angles ($0 \leq \theta \leq 4.5°$) are depicted in Fig. 2; it is clear that particles tend to travel further in the vertical direction

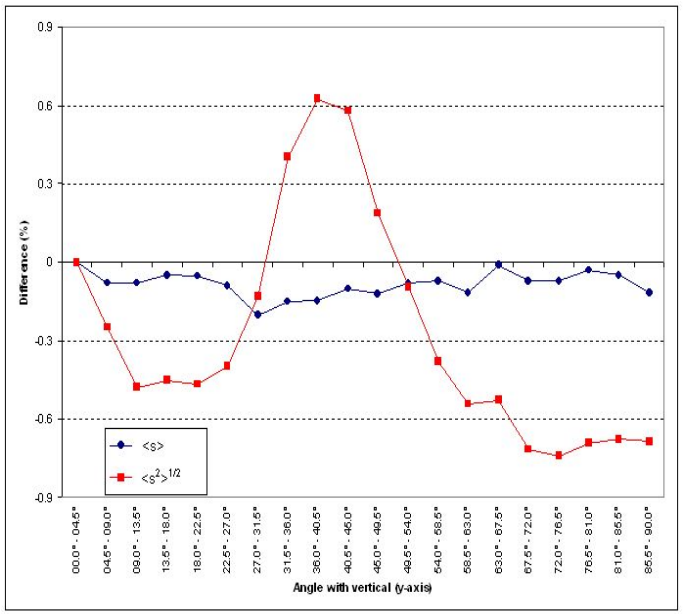

Figure 3. $\langle s\rangle$ and $\langle s^2\rangle^{1/2}$ at different angles

than in the horizontal direction. This anisotropic trend in the transport can also be seen when we examine $\langle s \rangle$ and $\langle s^2 \rangle$ in the same fashion; although the values of $\langle s \rangle$ remain fairly close to each other at all angles, it is clear that the same does not happen for $\langle s^2 \rangle$ (see Fig. 3).

3 GENERALIZED TRANSPORT THEORY

Consider a cylindrical pebble core with radius R and height Z, composed of spherical pebbles dropped into it in a "random" way. The gravitational force acting in the z-direction causes these pebbles to become arranged in a certain manner. The underlying question is: will the neutron transport in the z direction differ significantly from the x, y directions? To answer this question, we consider a transport equation for a hypothetical system in which the distance between collisions is not exponentially distributed.

3.1 The Generalized Boltzmann Equation

For the problem we want to approach, the incremental probability dp that a particle at point $\boldsymbol{x}$ with energy E will experience an interaction while traveling an incremental distance ds in a direction $\boldsymbol{\Omega}$ is given by $dp = \Sigma_t(\boldsymbol{x}, \boldsymbol{\Omega}, E)ds$. Here, Σ_t depends upon both s and $\boldsymbol{\Omega}$, since the locations of the scattering center in the system are correlated in a way that depends on the direction of flight $\boldsymbol{\Omega}$. For simplicity, we do not consider the most general problem here. We assume that:

- The physical system is infinite and statistically homogeneous.
- Particle transport is monoenergetic. (However, the inclusion of energy-dependence is straightforward.)
- Particle transport is driven by a known interior isotropic source $Q(\boldsymbol{x})$ satisfying $Q \to 0$ as $|\boldsymbol{x}| \to \infty$.
- $\Sigma_t(\boldsymbol{\Omega}, s)$ is known.
- The distribution function $P(\boldsymbol{\Omega} \cdot \boldsymbol{\Omega}')$ for scattering from $\boldsymbol{\Omega}'$ to $\boldsymbol{\Omega}$ is independent of s. (The correlation in the scattering center positions affects the distances to collision, but not the scattering properties when a collision occurs.)

Using the notation $\boldsymbol{x} = (x, y, z) =$ position and $\boldsymbol{\Omega} = (\Omega_x, \Omega_y, \Omega_z) =$ direction of flight (with $|\boldsymbol{\Omega}| = 1$), and defining

$$s = \text{the path length traveled by the particle since its previous interaction (birth or scattering)}, \tag{7}$$

we make the necessary adjustments in the theory presented by Larsen in [3], and without difficulty we obtain the *Generalized Boltzmann Equation*:

$$\frac{\partial \psi}{\partial s}(\boldsymbol{x}, \boldsymbol{\Omega}, s) + \boldsymbol{\Omega} \cdot \boldsymbol{\nabla} \psi(\boldsymbol{x}, \boldsymbol{\Omega}, s) + \Sigma_t(\boldsymbol{\Omega}, s)\psi(\boldsymbol{x}, \boldsymbol{\Omega}, s) = \delta(s)\, c \int_{4\pi} \int_0^\infty P(\boldsymbol{\Omega}' \cdot \boldsymbol{\Omega}) \Sigma_t(\boldsymbol{\Omega}', s') \psi(\boldsymbol{x}, \boldsymbol{\Omega}', s')\, ds' d\Omega' + \delta(s) \frac{Q(\boldsymbol{x})}{4\pi} \quad . \tag{8}$$

To repeat, we have for simplicity assumed an infinite homogeneous system with a "local" source $Q(\boldsymbol{x})$; and we take $\psi(\boldsymbol{x}, \boldsymbol{\Omega}, s) \to 0$ as $|\boldsymbol{x}| \to \infty$.

This equation can be written in a mathematically equivalent way, in which the delta function is not present. We write Eq. (8) for $s > 0$:

$$\frac{\partial \psi}{\partial s}(\boldsymbol{x}, \boldsymbol{\Omega}, s) + \boldsymbol{\Omega} \cdot \boldsymbol{\nabla} \psi(\boldsymbol{x}, \boldsymbol{\Omega}, s) + \Sigma_t(\boldsymbol{\Omega}, s)\psi(\boldsymbol{x}, \boldsymbol{\Omega}, s) = 0 \quad . \tag{9a}$$

Then, we operate on Eq. (8) by $\lim_{\varepsilon\to 0}\int_{-\varepsilon}^{\varepsilon}(\cdot)\,ds$ and use $\psi = 0$ for $s < 0$ to obtain:

$$\psi(\boldsymbol{x},\boldsymbol{\Omega},0) = c\int_{4\pi}\int_{0}^{\infty} P(\boldsymbol{\Omega}'\cdot\boldsymbol{\Omega})\Sigma_t(\boldsymbol{\Omega}',s')\psi(\boldsymbol{x},\boldsymbol{\Omega}',s')\,ds'd\Omega' + \frac{Q(\boldsymbol{x})}{4\pi}\quad . \tag{9b}$$

Eqs. (9) are mathematically equivalent to Eq. (8).

3.2 The Angular-dependent Path Length Distributions

Without loss of generality, let us consider a single particle, which is released from an interaction site at $x = 0$ in the direction $\boldsymbol{\Omega} = \boldsymbol{i}$ = direction of the positive x-axis. Eq. (9a) for this particle becomes:

$$\frac{\partial}{\partial s}\psi(x,\boldsymbol{\Omega}=\boldsymbol{i},s) + \frac{\partial}{\partial x}\psi(x,\boldsymbol{\Omega}=\boldsymbol{i},s) + \Sigma_t(\boldsymbol{\Omega}=\boldsymbol{i},s)\psi(x,\boldsymbol{\Omega}=\boldsymbol{i},s) = 0\quad . \tag{10}$$

For this particle, we have

$$x(s) = s \qquad \text{and} \qquad \psi(x(s),\boldsymbol{\Omega}=\boldsymbol{i},s) \equiv F(\boldsymbol{\Omega}=\boldsymbol{i},s)\quad . \tag{11a}$$

Therefore,

$$\frac{dF}{ds}(\boldsymbol{\Omega}=\boldsymbol{i},s) = \frac{\partial\psi}{\partial x}(x(s),\boldsymbol{\Omega}=\boldsymbol{i},s)\left(\frac{dx}{ds}\right) + \frac{\partial\psi}{\partial s}(x(s),\boldsymbol{\Omega}=\boldsymbol{i},s) = \frac{\partial\psi}{\partial x} + \frac{\partial\psi}{\partial s}\quad . \tag{11b}$$

Using this, Eq. (10) simplifies to:

$$\frac{dF}{ds}(\boldsymbol{\Omega}=\boldsymbol{i},s) + \Sigma_t(\boldsymbol{\Omega}=\boldsymbol{i},s)F(\boldsymbol{\Omega}=\boldsymbol{i},s) = 0\quad . \tag{12a}$$

We apply the initial condition

$$F(\boldsymbol{\Omega}=\boldsymbol{i},0) = 1\quad , \tag{12b}$$

because we are considering a single particle. The solution of Eqs. (12) is:

$$\begin{aligned} F(\boldsymbol{\Omega}=\boldsymbol{i},s) &= e^{-\int_0^s \Sigma_t(\boldsymbol{\Omega}=\boldsymbol{i},s')\,ds'} \\ &= \text{the probability that the particle will travel the distance} \\ &\quad s \text{ in the given direction } \boldsymbol{\Omega}=\boldsymbol{i} \text{ without interacting}\quad . \end{aligned} \tag{13}$$

Generalizing this equation for all directions, we obtain

$$\begin{aligned} F(\boldsymbol{\Omega},s) &= e^{-\int_0^s \Sigma_t(\boldsymbol{\Omega},s')\,ds'} \\ &= \text{the probability that the particle will travel the distance} \\ &\quad s \text{ in a given direction } \boldsymbol{\Omega} \text{ without interacting}\quad . \end{aligned} \tag{14}$$

The probability of a collision between s and $s + ds$ in a given direction $\boldsymbol{\Omega}$ is:

$$\Sigma_t(\boldsymbol{\Omega},s)F(\boldsymbol{\Omega},s)ds = p_{s|\boldsymbol{\Omega}}(s|\boldsymbol{\Omega})ds\quad , \tag{15}$$

and therefore:

$$\begin{aligned} p_{s|\boldsymbol{\Omega}}(s|\boldsymbol{\Omega}) &= \Sigma_t(\boldsymbol{\Omega},s)e^{-\int_0^s \Sigma_t(\boldsymbol{\Omega},s')\,ds'} \\ &= \text{conditional distribution function for the distance-to-collision} \\ &\quad \text{in a given direction } \boldsymbol{\Omega}\quad . \end{aligned} \tag{16}$$

Let us also define

$$p_{\mathbf{\Omega}}(\mathbf{\Omega})d\Omega = \text{probability that a particle is traveling in } d\Omega \text{ about } \mathbf{\Omega} \ ; \tag{17}$$

then

$$\begin{aligned} p(\mathbf{\Omega}, s)d\Omega ds = \ & (\text{probability that a particle is traveling in } d\Omega \text{ about } \mathbf{\Omega}) \times (\text{probability} \\ & \text{of a collision between } s \text{ and } s + ds \text{ in a given direction } \mathbf{\Omega}) \\ = \ & (p_{\mathbf{\Omega}}(\mathbf{\Omega})d\Omega)(p_{s|\mathbf{\Omega}}(s|\mathbf{\Omega})ds) \ ; \end{aligned} \tag{18}$$

that is, $p(\mathbf{\Omega}, s)$ is a joint distribution function.

From Eq. (16), the mean distance-to-collision (mean free path) in a given direction $\mathbf{\Omega}$ is:

$$\begin{aligned} \langle s_{\mathbf{\Omega}} \rangle(\mathbf{\Omega}) &= \int_0^\infty s p_{s|\mathbf{\Omega}}(s|\mathbf{\Omega}) \, ds \\ &= \int_0^\infty s \left[\Sigma_t(\mathbf{\Omega}, s) e^{-\int_0^s \Sigma_t(\mathbf{\Omega}, s')ds'} \right] ds \\ &= s \left[-e^{-\int_0^s \Sigma_t(\mathbf{\Omega}, s')ds'} \right]_0^\infty - \int_0^\infty \left[-e^{-\int_0^s \Sigma_t(\mathbf{\Omega}, s')ds'} \right] ds \\ &= \int_0^\infty e^{-\int_0^s \Sigma_t(\mathbf{\Omega}, s')ds'} \, ds \ . \end{aligned} \tag{19}$$

Hence, by the Law of Total Expectation [4], the mean free path $\langle s \rangle$ is given by

$$\langle s \rangle = \int_{4\pi} \int_0^\infty s p(\mathbf{\Omega}, s) ds d\Omega = \int_{4\pi} p_{\mathbf{\Omega}}(\mathbf{\Omega}) \langle s_{\mathbf{\Omega}} \rangle(\mathbf{\Omega}) d\Omega \ . \tag{20}$$

Note: for the rest of this work we assume that $\langle s_{\mathbf{\Omega}} \rangle(\mathbf{\Omega})$ is an even function of $\mathbf{\Omega}$. (From the physical point of view, the mean free path of a particle traveling in the direction $\mathbf{\Omega}$ must equal the mean free path of a particle traveling in the direction $-\mathbf{\Omega}$.)

3.3 Asymptotic Diffusion Limit of the GBE

To begin this discussion, we must first consider the Legendre-polynomial expansion of the distribution function $P(\mathbf{\Omega} \cdot \mathbf{\Omega}') = P(\mu_0)$:

$$P(\mu_0) = \sum_{n=0}^\infty \frac{2n+1}{4\pi} a_n P_n(\mu_0) \ , \tag{21}$$

where $a_0 = 1$ and $a_1 = \overline{\mu}_0$ = mean scattering cosine. We define $P^*(\mu_0)$ by:

$$P^*(\mu_0) = cP(\mu_0) + \frac{1-c}{4\pi} \ , \tag{22}$$

which has the Legendre polynomial expansion:

$$P^*(\mu_0) = \sum_{n=0}^\infty \frac{2n+1}{4\pi} a_n^* P_n(\mu_0) \ , \tag{23a}$$

$$a_n^* = \begin{cases} 1 & , \quad n = 0 \\ ca_n & , \quad n \geq 1 \end{cases} \ . \tag{23b}$$

Using the work in [5] as a guide, we scale $\Sigma_t = O(\varepsilon^{-1})$, $1-c = O(\varepsilon^2)$, $Q = O(\varepsilon)$, $P^*(\mu_0)$ is independent of ε, and $\partial\psi/\partial s = O(\varepsilon^{-1})$, with $\varepsilon \ll 1$. Eqs. (8) and (22) yield, in this scaling,

$$\frac{1}{\varepsilon}\frac{\partial\psi}{\partial s}(\boldsymbol{x},\boldsymbol{\Omega},s) + \boldsymbol{\Omega}\cdot\boldsymbol{\nabla}\psi(\boldsymbol{x},\boldsymbol{\Omega},s) + \frac{\Sigma_t(\boldsymbol{\Omega},s)}{\varepsilon}\psi(\boldsymbol{x},\boldsymbol{\Omega},s)$$
$$= \delta(s)\int_{4\pi}\int_0^\infty \left[P^*(\boldsymbol{\Omega}\cdot\boldsymbol{\Omega}') - \varepsilon^2\frac{1-c}{4\pi}\right]\frac{\Sigma_t(\boldsymbol{\Omega}',s')}{\varepsilon}\psi(\boldsymbol{x},\boldsymbol{\Omega}',s')\,ds'd\Omega' + \varepsilon\delta(s)\frac{Q(\boldsymbol{x})}{4\pi} \quad . \tag{24}$$

Next, we define define $\Psi(\boldsymbol{x},\boldsymbol{\Omega},s)$ by:

$$\psi(\boldsymbol{x},\boldsymbol{\Omega},s) \equiv \Psi(\boldsymbol{x},\boldsymbol{\Omega},s)\frac{e^{-\int_0^s \Sigma_t(\boldsymbol{\Omega},s')ds'}}{\langle s\rangle} \quad . \tag{25}$$

Then, using Eq. (16), Eq. (24) for $\psi(\boldsymbol{x},\boldsymbol{\Omega},s)$ becomes the following equation for $\Psi(\boldsymbol{x},\boldsymbol{\Omega},s)$:

$$\frac{\partial\Psi}{\partial s}(\boldsymbol{x},\boldsymbol{\Omega},s) + \varepsilon\boldsymbol{\Omega}\cdot\boldsymbol{\nabla}\Psi(\boldsymbol{x},\boldsymbol{\Omega},s)$$
$$= \delta(s)\int_{4\pi}\int_0^\infty \left[P^*(\boldsymbol{\Omega}\cdot\boldsymbol{\Omega}') - \varepsilon^2\frac{1-c}{4\pi}\right]p_{s|\boldsymbol{\Omega}}(s'|\boldsymbol{\Omega}')\Psi(\boldsymbol{x},\boldsymbol{\Omega}',s')\,ds'd\Omega'$$
$$+ \varepsilon^2\delta(s)\langle s\rangle\frac{Q(\boldsymbol{x})}{4\pi} \quad . \tag{26}$$

This equation is mathematically equivalent to:

$$\frac{\partial\Psi}{\partial s}(\boldsymbol{x},\boldsymbol{\Omega},s) + \varepsilon\boldsymbol{\Omega}\cdot\boldsymbol{\nabla}\Psi(\boldsymbol{x},\boldsymbol{\Omega},s) = 0 \quad , \quad s > 0 \ , \tag{27a}$$

$$\Psi(\boldsymbol{x},\boldsymbol{\Omega},0) = \int_{4\pi}\left[P^*(\boldsymbol{\Omega}\cdot\boldsymbol{\Omega}') - \varepsilon^2\frac{1-c}{4\pi}\right]\int_0^\infty p_{s|\boldsymbol{\Omega}}(s'|\boldsymbol{\Omega}')\Psi(\boldsymbol{x},\boldsymbol{\Omega}',s')ds'd\Omega'$$
$$+ \varepsilon^2\langle s\rangle\frac{Q(\boldsymbol{x})}{4\pi} \quad . \tag{27b}$$

Integrating Eq. (27a) over $0 < s' < s$, we obtain:

$$\Psi(\boldsymbol{x},\boldsymbol{\Omega},s) = \Psi(\boldsymbol{x},\boldsymbol{\Omega},0) - \varepsilon\boldsymbol{\Omega}\cdot\boldsymbol{\nabla}\int_0^s \Psi(\boldsymbol{x},\boldsymbol{\Omega},s')\,ds'$$
$$= \int_{4\pi}\left[P^*(\boldsymbol{\Omega}\cdot\boldsymbol{\Omega}') - \varepsilon^2\frac{1-c}{4\pi}\right]\int_0^\infty p_{s|\boldsymbol{\Omega}}(s'|\boldsymbol{\Omega}')\Psi(\boldsymbol{x},\boldsymbol{\Omega}',s')ds'd\Omega'$$
$$+ \varepsilon^2\langle s\rangle\frac{Q(\boldsymbol{x})}{4\pi} - \varepsilon\boldsymbol{\Omega}\cdot\boldsymbol{\nabla}\int_0^s \Psi(\boldsymbol{x},\boldsymbol{\Omega},s')\,ds' \quad . \tag{28}$$

Introducing into this equation the ansatz

$$\Psi(\boldsymbol{x},\boldsymbol{\Omega},s) = \sum_{n=0}^\infty \varepsilon^n\Psi^{(n)}(\boldsymbol{x},\boldsymbol{\Omega},s) \tag{29}$$

and equating the coefficients of different powers of ε, we obtain for $n \geq 0$:

$$\Psi^{(n)}(\boldsymbol{x},\boldsymbol{\Omega},s) = \int_{4\pi}P^*(\boldsymbol{\Omega}\cdot\boldsymbol{\Omega}')\int_0^\infty p_{s|\boldsymbol{\Omega}}(s'|\boldsymbol{\Omega}')\Psi^{(n)}(\boldsymbol{x},\boldsymbol{\Omega}',s')ds'd\Omega'$$
$$- \boldsymbol{\Omega}\cdot\boldsymbol{\nabla}\int_0^s \Psi^{(n-1)}(\boldsymbol{x},\boldsymbol{\Omega},s')\,ds'$$
$$- \frac{1-c}{4\pi}\int_{4\pi}\int_0^\infty p_{s|\boldsymbol{\Omega}}(s'|\boldsymbol{\Omega}')\Psi^{(n-2)}(\boldsymbol{x},\boldsymbol{\Omega}',s')ds'd\Omega'$$
$$+ \delta_{n,2}\langle s\rangle\frac{Q(\boldsymbol{x})}{4\pi} \quad . \tag{30}$$

We now solve these equations recursively, first for $n = 0$, then $n = 1$, etc. In doing this, we use the Legendre polynomial expansion (23) of $P^*(\mu_0)$.

Eq. (30) with $n = 0$ is:

$$\Psi^{(0)}(\boldsymbol{x}, \boldsymbol{\Omega}, s) = \int_{4\pi} P^*(\boldsymbol{\Omega} \cdot \boldsymbol{\Omega}') \int_0^\infty p_{s|\boldsymbol{\Omega}}(s'|\boldsymbol{\Omega}') \Psi^{(0)}(\boldsymbol{x}, \boldsymbol{\Omega}', s') ds' d\Omega' \quad . \tag{31}$$

The general solution of this equation is:

$$\Psi^{(0)}(\boldsymbol{x}, \boldsymbol{\Omega}, s) = \frac{\Phi^{(0)}(\boldsymbol{x})}{4\pi} \quad , \tag{32}$$

where $\Phi^{(0)}(\boldsymbol{x})$ is, at this point, undetermined.

Next, Eq. (30) with $n = 1$ is:

$$\Psi^{(1)}(\boldsymbol{x}, \boldsymbol{\Omega}, s) = \int_{4\pi} P^*(\boldsymbol{\Omega} \cdot \boldsymbol{\Omega}') \int_0^\infty p_{s|\boldsymbol{\Omega}}(s'|\boldsymbol{\Omega}') \Psi^{(1)}(\boldsymbol{x}, \boldsymbol{\Omega}', s') ds' d\Omega' - s\boldsymbol{\Omega} \cdot \boldsymbol{\nabla} \frac{\Phi^{(0)}(\boldsymbol{x})}{4\pi} \quad . \tag{33}$$

If $P^*(\boldsymbol{\Omega} \cdot \boldsymbol{\Omega}')$ is even (as is the case with isotropic scattering) this equation can easily be shown to have a particular solution of the form:

$$\Psi^{(1)}_{part}(\boldsymbol{x}, \boldsymbol{\Omega}, s) = -s\boldsymbol{\Omega} \cdot \boldsymbol{\nabla} \frac{\Phi^{(0)}(\boldsymbol{x})}{4\pi} \quad . \tag{34}$$

Hence, the general solution of Eq. (33) is:

$$\Psi^{(1)}(\boldsymbol{x}, \boldsymbol{\Omega}, s) = \frac{\Phi^{(1)}(\boldsymbol{x})}{4\pi} - s\boldsymbol{\Omega} \cdot \boldsymbol{\nabla} \frac{\Phi^{(0)}(\boldsymbol{x})}{4\pi} \quad , \tag{35}$$

where $\Phi^{(1)}(\boldsymbol{x})$ is undetermined.

We now consider Eq. (30) with $n = 2$. This equation has a solvability condition, which is obtained by operating by $\int_{4\pi} \int_0^\infty p_{s|\boldsymbol{\Omega}}(s|\boldsymbol{\Omega})(\cdot) ds d\Omega$. Using Eqs. (35) and (32) to obtain:

$$\int_0^s \Psi^{(1)}(\boldsymbol{x}, \boldsymbol{\Omega}, s')\, ds' = s \frac{\Phi^{(1)}(\boldsymbol{x})}{4\pi} - \frac{s^2}{2} \boldsymbol{\Omega} \cdot \boldsymbol{\nabla} \frac{\Phi^{(0)}(\boldsymbol{x})}{4\pi} \quad , \tag{36a}$$

and:

$$\int_{4\pi} \int_0^\infty p_{s|\boldsymbol{\Omega}}(s'|\boldsymbol{\Omega}') \Psi^{(0)}(\boldsymbol{x}, \boldsymbol{\Omega}', s')\, ds' d\Omega' = \Phi^{(0)}(\boldsymbol{x}) \quad , \tag{36b}$$

the solvability condition becomes:

$$\begin{aligned} 0 =& \frac{1}{4\pi} \int_{4\pi} \int_0^\infty p_{s|\boldsymbol{\Omega}}(s|\boldsymbol{\Omega}) \frac{s^2}{2} (\boldsymbol{\Omega} \cdot \nabla)^2 \Phi^{(0)}(\boldsymbol{x})\, ds d\Omega \\ & - \frac{(1-c)}{4\pi} \int_{4\pi} \int_0^\infty p_{s|\boldsymbol{\Omega}}(s|\boldsymbol{\Omega}) \Phi^{(0)}(\boldsymbol{x})\, ds d\Omega + \langle s \rangle Q(\boldsymbol{x}) \quad . \end{aligned} \tag{37a}$$

Thus

$$0 = \frac{1}{2\langle s \rangle} \frac{1}{4\pi} \int_{4\pi} \langle s^2_{\boldsymbol{\Omega}} \rangle (\boldsymbol{\Omega}) (\boldsymbol{\Omega} \cdot \nabla)^2 \Phi^{(0)}(\boldsymbol{x})\, d\Omega - \frac{(1-c)}{\langle s \rangle} \Phi^{(0)}(\boldsymbol{x}) + Q(\boldsymbol{x}) \quad . \tag{37b}$$

Evaluating the angular integrals and rearranging, we obtain the following anisotropic diffusion equation for $\Phi^{(0)}(\boldsymbol{x})$:

$$-\mathrm{D}_x \frac{d^2}{dx^2}\Phi^{(0)}(\boldsymbol{x}) - \mathrm{D}_y \frac{d^2}{dy^2}\Phi^{(0)}(\boldsymbol{x}) - \mathrm{D}_z \frac{d^2}{dz^2}\Phi^{(0)}(\boldsymbol{x}) + \frac{1-c}{\langle s\rangle}\Phi^{(0)}(\boldsymbol{x}) = Q(\boldsymbol{x}), \tag{38}$$

where

$$\mathrm{D}_x = \frac{1}{2\langle s\rangle}\left(\frac{1}{4\pi}\int_{4\pi}\langle s^2_{\boldsymbol{\Omega}}\rangle(\boldsymbol{\Omega})\Omega_x^2 d\Omega\right), \tag{39a}$$

$$\mathrm{D}_y = \frac{1}{2\langle s\rangle}\left(\frac{1}{4\pi}\int_{4\pi}\langle s^2_{\boldsymbol{\Omega}}\rangle(\boldsymbol{\Omega})\Omega_y^2 d\Omega\right), \tag{39b}$$

$$\mathrm{D}_z = \frac{1}{2\langle s\rangle}\left(\frac{1}{4\pi}\int_{4\pi}\langle s^2_{\boldsymbol{\Omega}}\rangle(\boldsymbol{\Omega})\Omega_z^2 d\Omega\right). \tag{39c}$$

To summarize: if $P^*(\boldsymbol{\Omega}\cdot\boldsymbol{\Omega}')$ is even, the solution $\psi(\boldsymbol{x},\boldsymbol{\Omega},s)$ of Eq. (24) satisfies:

$$\psi(\boldsymbol{x},\boldsymbol{\Omega},s) = \frac{\Phi^{(0)}(\boldsymbol{x})}{4\pi}\frac{e^{-\int_0^s \Sigma_t(\boldsymbol{\Omega},s')ds'}}{\langle s\rangle} + O(\varepsilon) \ , \tag{40}$$

where $\Phi^{(0)}(\boldsymbol{x})$ satisfies Eq. (38). Also, integrating Eq. (40) over $0 < s < \infty$ and $\boldsymbol{\Omega} \in 4\pi$, and using equation (19), we obtain to leading order:

$$\int_{4\pi}\psi(\boldsymbol{x},\boldsymbol{\Omega})\,d\Omega = \Phi^{(0)}(\boldsymbol{x})\frac{1}{4\pi\langle s\rangle}\int_{4\pi}\langle s_{\boldsymbol{\Omega}}\rangle(\boldsymbol{\Omega})d\Omega \ , \tag{41}$$

where $\psi(\boldsymbol{x},\boldsymbol{\Omega})$ is the classic angular flux.

It is easy to show that if s and $\boldsymbol{\Omega}$ are independent random variables, then $\mathrm{D}_x = \mathrm{D}_y = \mathrm{D}_z$ and Eq. (38) reduces to the result obtained in [3]. From there, one can show that if the pathlength distribution is exponential, Eq. (38) reduces to the classic diffusion equation, as it must.

4 GENERALIZED TRANSPORT THEORY: 2-D CASE

For the "Flatland" 2-D case, Eq. (38) becomes

$$-\mathrm{D}_x \frac{d^2}{dx^2}\Phi^{(0)}(\boldsymbol{x}) - \mathrm{D}_y \frac{d^2}{dy^2}\Phi^{(0)}(\boldsymbol{x}) + \frac{1-c}{\langle s\rangle}\Phi^{(0)}(\boldsymbol{x}) = Q(\boldsymbol{x}), \tag{42}$$

where

$$\mathrm{D}_x = \frac{1}{2\langle s\rangle}\left(\frac{1}{2\pi}\int_0^{2\pi}\langle s^2_{\boldsymbol{\Omega}}\rangle(\boldsymbol{\Omega})\cos^2(\varphi)d\varphi\right), \tag{43a}$$

$$\mathrm{D}_y = \frac{1}{2\langle s\rangle}\left(\frac{1}{2\pi}\int_0^{2\pi}\langle s^2_{\boldsymbol{\Omega}}\rangle(\boldsymbol{\Omega})\sin^2(\varphi)d\varphi\right). \tag{43b}$$

The same manipulation described in Section 2 applied to Eq. (42) yields:

$$\langle \rho^2\rangle = \frac{2}{\Sigma_a}(\mathrm{D}_x + \mathrm{D}_y), \tag{44a}$$

$$\langle x^2\rangle = 2\frac{\mathrm{D}_x}{\Sigma_a}, \tag{44b}$$

$$\langle y^2\rangle = 2\frac{\mathrm{D}_y}{\Sigma_a}. \tag{44c}$$

Table II. Prediction of the Non-classical Model with Angular Dependence

	Numerical Results	Theoretical Predictions		Relative Error (Compared to Numerical Results)	
		Atomic Mix	New Theory	Atomic Mix	New Theory
$\langle \rho^2 \rangle^{1/2}$	17.42908	17.33835	17.43655	0.52056%	0.04286%
$\langle x^2 \rangle^{1/2}$	12.29878	12.26006	12.31386	0.31479%	0.12258%
$\langle y^2 \rangle^{1/2}$	12.34961	12.26006	12.34513	0.72507%	0.03630%

Using the experimentally-obtained values for $\langle s^2 \rangle$ in Table I (and doing a Riemann sum to calculate the diffusion coefficients), Eqs. (44) generate predictions for $\langle x^2 \rangle$ and $\langle y^2 \rangle$ that reflect the anisotropic behavior we expect, as can be seen in Table II.

We note that the new angular-dependent theory produces (i) an estimate of $\langle \rho^2 \rangle^{1/2}$ that is more than one order of magnitude more accurate than the atomic mix estimate, and (ii) estimates of $\langle x^2 \rangle^{1/2}$ and $\langle y^2 \rangle^{1/2}$ that are significantly more accurate than the atomic mix estimates. These results indicate that by including angle-dependence in the probability distribution function for distance to collision, the generalized transport theory can accurately estimate even small anisotropic effects in neutron distributions.

5 CONCLUSIONS

The modeling of neutron transport in random media has been limited to a few special techniques, such as the atomic mix approximation and the Levermore-Pomraning model, which is known to be inaccurate when applied to diffusive problems [2]. This paper shows that, at least for the kind of problem treated here, the generalized transport theory yields more accurate results than atomic mix, and it accurately predicts anisotropic diffusion in this kind of system.

Finally, we acknowledge that even though the 2-D problem considered above exhibits only small deviations from the atomic mix model and small anisotropic effects, we expect that both of these these features will be greater for 3-D problems. If correct, this will increase the importance of a mathematical model that is capable of describing these features. We have two main reasons for this expectation:

- (i) The packing fraction in 3-D tends to be about 0.14 smaller than in the 2-D case, meaning that the void percentage of the system is larger in the 3-D case;

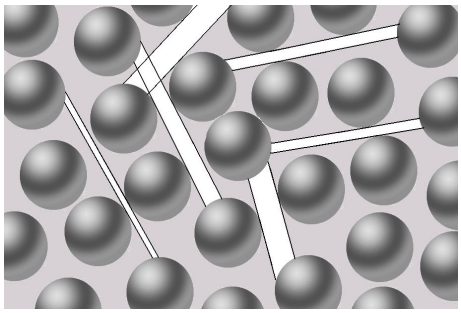

Figure 4. Horizontal void corridors in a layer of spheres in a 3-D system

- (ii) While "void corridors" in the 2-D case are in general smaller than the diameter of a disc in both horizontal and vertical directions, the same will not be true in the 3-D case. In fact, the horizontal directions of spherical packing will have numerous "void corridors", with lengths larger than that of a sphere diameter d (Fig. 4). Due to the effect of gravity, these corridors will generally not be bigger than d in the vertical direction. Previous results showing anisotropic distributions in 3-D packings obtained by a similar method [1] seem to confirm this expectation.

ACKNOWLEDGEMENTS

R. Vasques would like to thank CAPES - Coordenação de Aperfeiçoamento de Pessoal de Nível Superior and the Fulbright Program for finantial and administrative support.

REFERENCES

[1] A. Pavlovitch, R. Jullien, P. Meakin, "Geometrical Properties of a Random Packing of Hard Spheres," *Physica A*, **176**, pp. 206-219 (1991).

[2] E. W. Larsen, R. Vasques, M. T. Vilhena, "Particle Transport in the 1-D Diffusive Atomic Mix Limit," *Proc. International Topical Meeting on Mathematics and Computation, Supercomputing, Reactor Physics and Nuclear and Biological Applications, M&C 2005*, Avignon, France (2005), on CD-ROM.

[3] E. W. Larsen, "A Generalized Boltzmann Equation for 'Non-Classical' Particle Transport," *Proc. International Topical Meeting on Mathematics & Computation and Supercomputing in Nuclear Applications, M&C+SNA 2007*, Monterey, California (2007), on CD-ROM.

[4] P. Billingsley, *Probability and Measure*, John Wiley & Sons, New York (1995).

[5] E.W. Larsen, J.E. Morel, and J.M. McGhee, "Asymptotic Derivation of the Multigroup P_1 and Simplified P_N Equations with Anisotropic Scattering," *Nucl. Sci. Eng.* **123**, 328 (1996).